BeBeC-2016-D2

REDUCTION OF THE HYDRODYNAMIC NOISE ON A BEAMFORMING ARRAY

Máté Szőke[1] and Mahdi Azarpeyvand[1]
[1]Aeroacoustics and Aerodynamics Research Group, Faculty of Engineering
University of Bristol, Queens Building, University Walk, BS8 1TR, Bristol, United Kingdom

Abstract

The design and build process of an 80 microphone beamforming array is reported. The array is designed to be installed on the wall of a large closed circuit wind tunnel, primarily for helicopter rotor noise measurement and source identification studies. The acoustic data collected using the array is prone to contamination due to the presence of a strong hydrodynamic field on the wall of the wind tunnel, caused by the wall boundary layer and also the down-wash flow from the helicopter rig. A study has been carried out for the reduction of the hydrodynamic noise using different stainless steel wire-mesh materials, recessing the microphones behind the screen and adding porous foam material in the space behind the screen and microphones. The effect of these treatments are investigated and evaluated for a number of test cases. In addition, different beamforming algorithms, such as the delay-and-sum and functional beamforming are used and compared in this study for different type of noise sources over the entire frequency range of interest. The designed array can deliver a dynamic range of 13-15 dB and low sidelobe levels.

1 INTRODUCTION

Aerodynamic related measurements, such as aerodynamic loading and flow visualization, are usually carried out in closed section wind tunnels, while aeroacoustic tests are preferably done in open-section anechoic wind tunnels. The main aeroacoustic limitation of the open-section tunnels comes from the background noise due to jet flow, particularly at high velocities. High flow velocities can be achieved in closed section wind tunnels, which from an acoustic point of view is not an ideal environment for acoustic and beamforming measurements. In such cases, the microphones are usually mounted on the wall of the wind tunnel, where the presence of strong hydrodynamic fluctuations, mainly due to the presence of the boundary layer, swamp the acoustic signal and leads to the contamination of the data.

The effect of such pressure fluctuations can be reduced by increasing the number of microphones, which inevitably leads to cost increase and larger space requirements. Increasing the data acquisition time also reduces the influence of these fluctuations. Subtracting out the background noise is a well defined approach [3], which on the other hand still requires multiple test-runs to achieve a statistically reliable result.

The physical separation of the flow from the microphones have been studied before [6, 12], and such approaches have been widely used [10, 11, 13]. In these cases, the beamforming array is recessed behind a stretched fabric. This material must satisfy the following requirements: It shall (a) be acoustically transparent, (b) filter out the hydrodynamic noise field, (c) preserve the acoustic noise signal and (d) have sufficient mechanical resistance. The most widely used material for this purpose is Kevlar, which is usually installed such that it is flush mounted on the side of the wind tunnel. The microphones are mounted behind the Kevlar with a given recess depth. It has been reported that this layout gives a reasonably low acoustic loss, while the drawback of the layout is that the flow might interact with the filaments of the Kevlar which in turn results in high frequency noise [8]. This flow-induced high frequency noise can affect the quality of the data at high frequencies, which is of particular interest for noise mapping of scaled models. The use of woven wire-mesh cloth has also been suggested, for example by Fleury *et al.* [8] and it has been reported that with a carefully chosen wire-mesh, one can effectively reduce the hydrodynamic noise without the emergence of flow-induced high frequency noise.

In this paper, we further investigate the use of woven meshes to reduce the hydrodynamic noise field. Prior research [8] had shown that the use of Dutch twilled woven wire-mesh gives reasonably good results for the reduction of the unwanted pressure fluctuations, however the effect of different wire-meshes with different properties (pore sizes, directionality, transparency) of this particular material has not yet been studied. As a first step, three different wire-meshes have been investigated in the closed-circuit low turbulence wind tunnel at the University of Bristol. The effects of the stretching direction of the materials with respect to the flow and the recess depth of the microphones behind the mesh are also studied. From the presented test cases a layout is chosen as the most effective for hydrodynamic noise reduction, and will be applied to a recently designed and built 80 microphone beamforming array. The array design and build will be discussed in Section 3.

As a second step, a beamforming array is designed in the framework of the National Rotor Rig Project. The main purpose is to construct an 80 microphone array for helicopter rotor noise measurements. A helicopter rig is built in the framework of the project, with rotor span of 1.8 m and blade rotation speed of 3000 RPM, equivalent to a tip velocity of approximately 280 m/s (Mach number of $\approx$0.8). The rig will be installed in the De Havilland Tunnel at the University of Glasgow, where tests will be carried out with wind speeds of up to 80 m/s. This configuration poses challenges both in terms of the design of the beamforming array and the post-processing of the acquired data. Due to the wind speed and the down-wash flow from the helicopter rotor, special care has to be taken during the beamforming array design for the reduction of the hydrodynamic noise. This is addressed with the application of woven wire-mesh material and recessing of the microphones behind the mesh, which will be discussed in Section 2. The measurements will include high speed rotating sources, and it will also have to take into consideration the non-anechoic conditions of the tunnel. Appropriate signal processing method will be employed to address these issues.

2 WALL HYDRODYNAMIC NOISE REDUCTION

In this section, the reduction of wall hydrodynamic noise is addressed. A small rig was built to study the reduction of the wall hydrodynamic noise field. The rig consists of 7 microphones, 5 of which installed behind exchangeable wire meshes and the recess depth of the microphones distance behind the wire mesh can be adjusted. The remaining two microphones were mounted flush upstream and downstream of the wire mesh, see Fig. 1. The rig was mounted on the wall of the closed circuit low turbulence wind tunnel at the University of Bristol [4]. The properties of the wire meshes will be discussed in subsection 2.1.

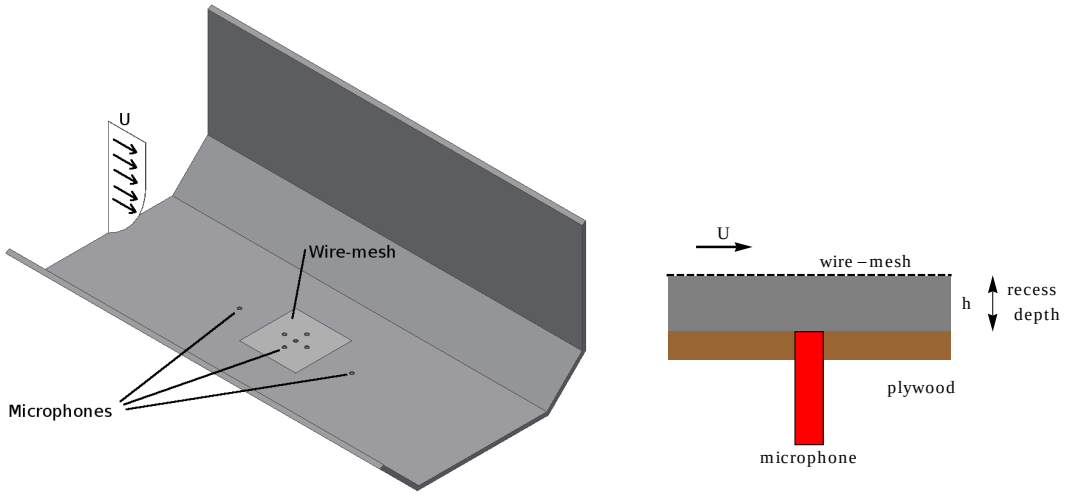

(a) The stretch rig in the wind tunnel (b) Cross section of the rig

Figure 1: Layout of the hydrodynamic noise reduction tests

Three different stainless steel Dutch twilled weave wire meshes have been tested. The properties of these materials are listed in Table 1. The three different wire meshes are referred to as WM1, WM2 and WM3 in the followings. The wire meshes are manufactured by GKD UK Ltd. The original purpose of these wire-meshes is to filter different types of fluids, where a reasonably high pressure difference drives the filtration process. The structure of a sample wire-mesh is shown in Fig. 2. The figure shows that the material is made of filaments woven perpendicularly to each other, where the vertical and horizontal filaments are referred to as the warp and the weft filaments respectively, see Fig. 2.

The first wire-mesh (WM1) is much thicker than the other two, leading to much higher tensile strength. Therefore, the surface of the first material is also rougher compared to the other two, which may result in interaction between the turbulence present in the boundary layer with the filaments.

2.1 Tested wire-meshes

The acoustic transparency of these materials depends on their pores which are triangular in shape and formed between the weft filaments, see Fig. 2. In our case, the materials have been chosen such that the number of filaments in the warp direction gradually increases to achieve

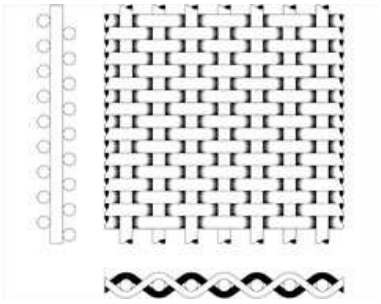

Figure 2: Dutch twill weave mesh structure [9]

different pore sizes. From an acoustical point of view, it has been proven that these materials are acoustically transparent with an attenuation loss of 2-3 dB [8]. In the current tests, the effect of pores size and material type on the noise reduction level and any potential broadband and tonal noise contamination is investigated. Two scenarios were considered: (a) when the area of the pores are parallel and (b) when the pores are perpendicular to the wind speed.

The wire-meshes are fully stretched by the rig to avoid any vibration of the meshes above the microphones, which ensures that the pressure measurements are not contaminated by any noise related to the motion of the wire-mesh. From the mechanical point of view, it is important to note that the maximum elongation in the weft direction that these materials can withstand without tearing is approximately 3-5 %. The other drawback of these materials is that they are highly sensitive to local mechanical impacts (for example scratches), therefore extra care needs to be taken during the handling and stretching process.

Table 1: Dutch twilled weave wire mesh properties

	Number of filaments		Pore size	Thickness	Tensile strength [N/mm]	
	Warp dir.	Weft dir.	[μm]	[mm]	Warp dir.	Weft dir.
Mesh 1	80	700	47	0.256	18.9	82.6
Mesh 2	165	1400	21	0.146	15.6	48.4
Mesh 3	200	1400	15	0.143	23.9	45.7

2.2 Test set-up

In order to test the hydrodynamic noise reduction capability of the wire-meshes listed in Table 1, a test rig has been built to hold and fully stretch the wire-mesh, see Fig. 1. As seen in Fig. 1(a), microphones are located beneath the wire-mesh and the space between the microphones and the wire-mesh is filled with porous foam. The rig has been flush mounted on the wall of a low turbulence wind tunnel with a hexagonal cross section. The layout of the rig installed in the tunnel is shown in Fig. 1(a). Five microphones have been installed 30 mm from each other forming a cross shape, see Fig. 1(a). Two additional microphones were flush mounted upstream and downstream of the rig, 150 mm from the centre microphone in the cross shape.

The microphones used in this experiment are the G.R.A.S. 40PL high pressure microphones with a maximum of 150 dB dynamic range.

The microphones were recessed behind the stretched wire-mesh, as shown schematically in Fig. 1(b). The space between the stretched material and the microphone has been filled with polypropylene acoustic foam with a typical pore number of 80 PPI (pores per inch). The recess depth is noted by h and has been set to 2, 7 and 13 mm (small, medium and large). The direction of stretching can be changed by rotating the rig 90° relative to the flow direction. The effective area of the stretched wire mesh is 150 mm $\times$ 150 mm.

Tests have been carried out for wind speeds of 20, 30, 40 and 50 m/s. A loudspeaker was installed flush mounted to the wall of the tunnel opposite to the rig behind a WM2 type material. The speaker is used to produce different type of noises inside the wind tunnel and test the acoustic transparency of the wire meshes. The data was recorded for 32 seconds using the National Instrument PXIe-4499 cards, with a sampling frequency of 204,800 Hz. The applied frequency resolution in the post-processing was Δf = 64 Hz.

2.3 Hydrodynamic noise reduction results

As a first step, the different wire-meshes have been investigated at different flow speeds inside the wind tunnel. The tunnel has not been treated acoustically and therefore has strong acoustic tones that are clearly identifiable in the sound spectra. The power spectrum of the pressure data are plotted in Figs. 3 to 5. The sensitivity of the microphones drops approximately 5 dB at 20 kHz, and above 30 kHz the results become flat and non-reliable. The black curves in the following figures always represent the results of the flush mounted microphone upstream of the rig, while the coloured curves are obtained by averaging the data from the five recessed microphones.

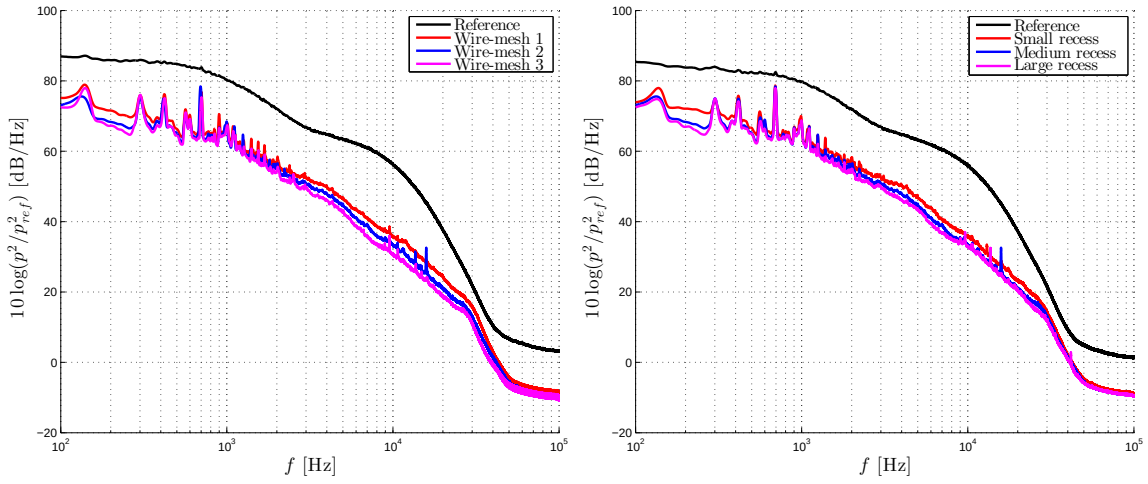

(a) The comparison of the three different wire-meshes

(b) The effect of recess depth

Figure 3: The comparison of the noise reduction of the wire meshes at 40 m/s wind speed (a) and the effect of recess depth on WM2 at 40 m/s wind speed (b)

Figure 3 shows the comparison of the noise reduction obtained using different wire meshes

(Fig. 3(a)) and the effect of the changes to the recess depth (Fig. 3(b)) at 40 m/s. The acoustic results from the wind tunnel showed the lowest number of tonal peaks at 40 m/s, while the trend of the noise reduction was found to be the same at all wind speeds, therefore only the 40 m/s case is shown here.

By comparing the three different wire meshes, we can see that they show similar behaviour to each other. The tones of the wind tunnel in the region of 300-900 Hz are clearly visible for all the cases, while they remain hidden in the reference microphones data, which is contaminated by the hydrodynamic noise. This means that the hydrodynamic noise has been successfully reduced using the wire-meshes. To quantify the results, the overall sound pressure levels (L_p) have been calculated for all the four lines, from which the noise reduction (ΔL_p) was calculated. The L_p calculation was performed between 100 Hz and 30 kHz and the noise reduction achieved with WM1, WM2 and WM3 was 12.8, 14.2 and 14.7 dB, respectively. It can therefore be concluded that the noise reduction level increases by decreasing the pore size of the wire-mesh. These results suggest that, bearing in mind that the difference between WM2 and WM3 is only 0.5 dB, and the third material is significantly weaker and more fragile, the use of the second material is rather more practical.

The effect of the recess depth on the power spectra has also been investigated. Figure 3(b) shows the effect of microphone recess depth for the WM2 case at 40 m/s wind speed. The results show that increasing the recess depth can improve the proper capture of the tones over the entire frequency range, particularly at low frequencies. The calculated sound pressure level reductions for the three different recess depths compared to the reference microphone are 11.35, 12.80 and 13.47 dB, respectively. It is evident from the results that the use of small recess depth gives less clear tonal peaks.

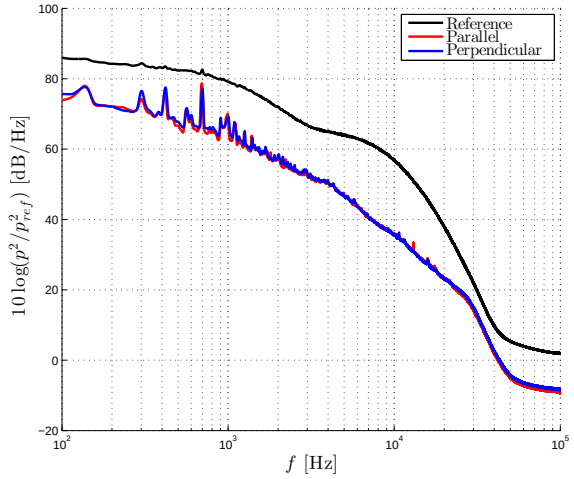

Figure 4: Directional sensitivity of the wire-mesh: WM2 stretched parallel and perpendicular to the flow

The interaction of the boundary layer with the pores and the wire-mesh filaments and its potential impact on the hydrodynamic noise reduction has also been investigated. Figure 4 shows the results for WM2 in two configurations: (a) when the areas defined by the pores were parallel with the flow and (b) when these areas were perpendicular to the flow. Results have been obtained for microphones with medium recess depth (7 mm) at 40 m/s. For the case when the

pores were parallel with the flow the tones are slightly clearer than when the pores were facing perpendicular to the flow. There are slight differences between the tones at low frequencies (100 – 900 Hz), while all the higher frequencies show almost identical results. It has therefore been concluded that the parallel stretch is slightly more effective than the perpendicular configuration.

To test the acoustic transparency of the wire-meshes, a test has been carried out using a loudspeaker mounted on the opposite side of the rig. The acoustic transparency of the wire meshes has been investigated for the following cases: (a) at non-zero flow conditions (40 m/s) the speaker has been turned on and its volume has been set such that the speaker is approximately as loud as the background noise and (b) the wind tunnel was turned off while the speaker had the same volume as in case (a). In this test, the loudspeaker was excited at 7 kHz. From the results in Fig. 5 , it is clearly visible that the wire-mesh is highly transparent, and the tone stands out significantly more for the microphones recessed behind the wire-mesh. The calculated ΔL_p for this case is 10.82 dB. In Fig. 5(b) the flow velocity is zero (the tunnel was turned off, and therefore no hydrodynamic noise) while the 7 kHz tone was still emitted from the speaker. The two curves are almost identical, with only some negligible losses present at low frequencies. This case allows to approximate the attenuation of the pressure signals through the wire mesh, which was 2.05 dB, which is in agreement with the finding of Fleury *et al.* [8] who reported a typical attenuation of 2.5 dB for a similar material.

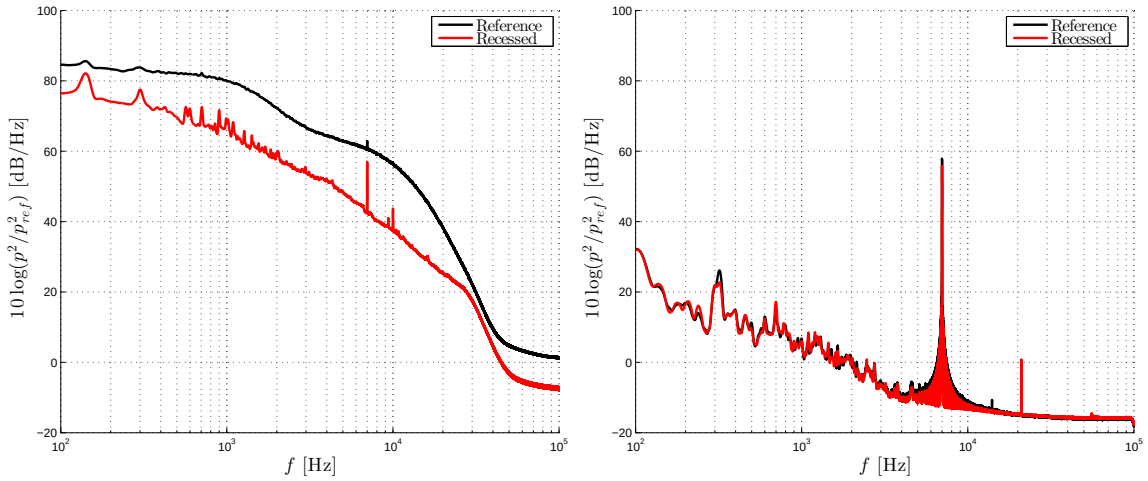

(a) 40 m/s, medium recess depth

(b) 0 m/s, medium recess depth

Figure 5: Transparency test on WM2, the speaker was emitting 7 kHz tonal noise

Based on the results presented in this section, it is evident that the choice wire-mesh, pore size, direction of the filament and recess depth can have some effects on the detection of tonal noises and the reduction of the broadband hydrodynamic noise. Also, considering the mechanical properties of the wire-mesh investigated in this study, it was concluded that WM2 can provide the best acoustic and mechanical performance.

3 ARRAY DESIGN

This section describes the process of the design and build of an 80 element beamforming array for a helicopter rotor rig in a closed circuit wind tunnel. Based on the results obtained in Section 2, it has been concluded that the layout with the WM2 wire-mesh, microphone recess depth of 7 mm and wire-mesh stretched in the direction of the flow gives the most appropriate results for beamforming application. In this section, we shall first introduce the design aims and constraints, describe the array layout and finally present the assembly and preliminary test results for some simple noise sources.

3.1 Design aims and limitations

The main purpose of the array is to measure and study helicopter rotor rig noise sources. The array will be mounted in the De Havilland Tunnel (United Kingdom National Wind Tunnel Facility) at the University of Glasgow. The test section of the tunnel is 9' $\times$ 7' (2.7 m $\times$ 2.1 m) with an octagonal cross-section shape. The maximum achievable flow speed in the tunnel is 80 m/s. The rotor plane of the test rig is planned to be installed 1.8 m above the floor of the tunnel. This means that the array must be mounted either on the floor or the ceiling (below or above the rotor plane). The available space for the array on the walls of the wind tunnel is 1 m $\times$ 1 m. The array will be placed on the advancing side of the blades.

The microphones chosen for this array are the G.R.A.S. 40PL piezoelectric constant current powered (CCP) microphones. They can deliver a large dynamic range which makes them a suitable candidate for this array. The microphones are powered by the data acquisition hardware (National Instruments PXIe-4499), which supports the use of CCP microphones.

3.2 Microphone layout

The array structure has been designed such that if the layout needs to be changed in the future, it can be done easily. The layout of the array is based on the widely used logarithmic spiral method. An example of the logarithmic arms is shown in Fig. 6(a). The microphones are distributed along several logarithmic arms such that each microphone senses an equal aperture area. The radial and polar coordinates of the microphones can be described by the following equations:

$$r_{m,i} = r_0 \mathrm{e}^{\theta \cot \nu}, \tag{1}$$

$$A_i = (r_{c,i-1}^2 - r_{c,i}^2)\pi, \tag{2}$$

$$r_{m,i} = \frac{r_{c,i-1} - r_{c,i}}{2}, \tag{3}$$

where $r_{m,i}$ is the radius of the i$^{\text{th}}$ microphone, r_0 is the initial radius of the logarithmic arms, θ is the angle of the i$^{\text{th}}$ microphone in the polar coordinate system, ν describes the "curviness" of the logarithmic arms, A_i denotes the equal aperture areas defined between two neighbouring blue circles in Fig. 6(a), and $r_{c,i}$ is the radius of the i$^{\text{th}}$ blue circle. The sensors are represented by blue dots, the logarithmic arms are shown by red curves, and the inner and outer diameters of the logarithmic spiral are denoted by r_0 and r_{Out} in Fig. 6(a).

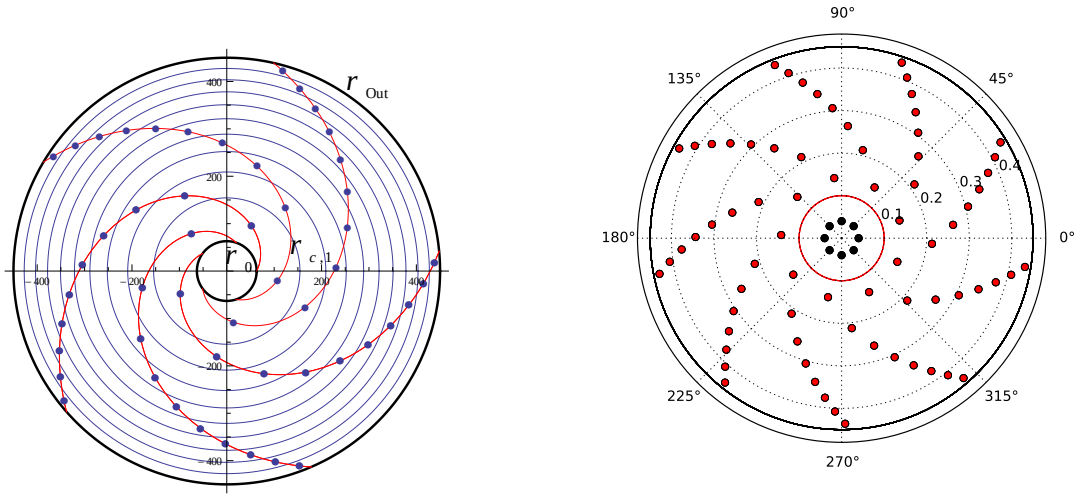

(a) An example for equal aperture area weighting of microphones

(b) The final array layout: 9 arms with 8 microphones on each arm with an additional 8 microphones populated in the centre of the array

Figure 6: Array layouts

In order to have the wire mesh stretched above the microphones, a metal frame was required which slightly decreased the available space for the beamforming array to a circular space with a diameter of $D = 950$ mm.

Odd number of arms have been considered to avoid the redundancy of the layout [2]. As shown in Fig. 6(b), the array consists of a number of microphones distributed along the arms and a number of microphones at the centre of the array. By populating microphones in the centre of the array, an inner radii weighting was achieved, while the formerly discussed equal aperture weighting yields to an outer radii weighting [2]. The combination of this two is expected to result in better dynamic range and lower number of sidelobes [2], compared to the layouts where the microphones are distributed with an equal arc-length along one or more logarithmic spirals.

A number of different array layouts have been considered and beamforming measurements have been simulated with the aid of Acoular [1], which is an open source beamforming platform. The basic delay-and-sum beamforming algorithm has been applied to calculate the beamforming results. We have simulated (a) a single noise source, (b) two noise sources separated from each other with a given distance and (c) distribution of point sources, forming a line source. In each case, these noise sources were emitting 100 dB white noise. This parametric study formed the basis for finding the array layout with acceptable dynamic range and minimum number of sidelobes. We considered different number of arms (3, 5, 7, 9, 11), varied the inner radius ($r_0 = 0.05 \ldots 0.15$ m) and the "curviness" of the arms ($\nu = 0.4 \ldots 1.55$) in the simulations. The best results were achieved with the layout of 9 arms and 8 microphones distributed along each arm, with an extra 8 microphones located at its centre. The layout of this array is presented in Fig. 6(b). The central microphones are shown with black dots and those laid out along the logarithmic arms are shown with red dots.

The simulated delay-and-sum beamforming results of this array are shown in Figs. 7 and 8.

Figure 7(a) shows the noise map at 8 kHz for a single white noise source located one meter from the array centre, and Fig. 7(b) shows the beamforming maps at 8 kHz for two white noise sources of the same kind located such that the array sees them 15° from each other. Figure 8(a) shows the noise map evaluated at 8 kHz for a line white noise source formed using a fine distribution of point white noise sources. Figure 8(b) shows the two sources case was evaluated at the Raleigh resolution limit [10], which for this configuration is evaluated at 1800 Hz. From these plots we can see that the array can reach up to 15 dB dynamic range and the observed sidelobes have a reasonably low level of about 13-15 dB below the main noise source. Based on these results, we expect the array to achieve a good dynamic range with low sidelobe levels and that it can distinguish different noise sources at the Raleigh resolution limit, which might be further improved using different beamforming methods.

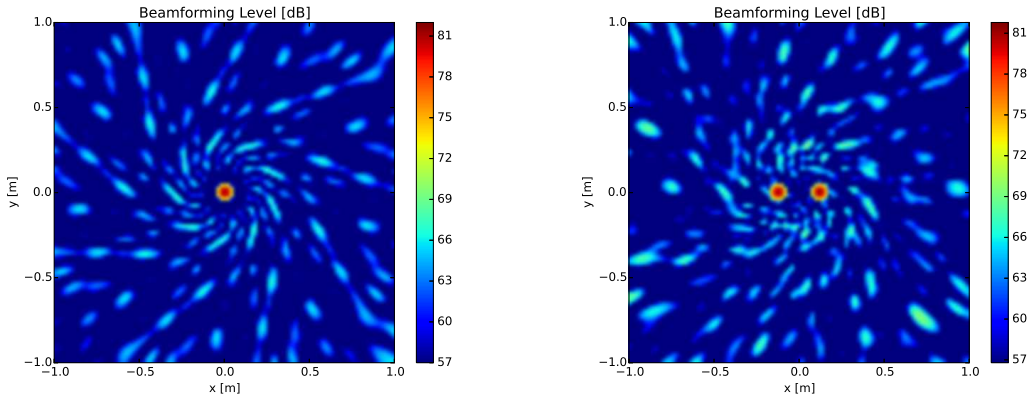

(a) A single noise source emitting white noise: beamforming map shown at 8 kHz

(b) Two noise sources emitting white noise: beamforming map shown at 8 kHz

Figure 7: Simulated results of the best performing array

3.3 Beamforming array build

In the final stage, the beamforming array was built and its performance was tested for a variety of noise sources. The array has a frame on which the wire mesh is mounted and it is supposed to bring and hold the mesh in tension. The elongation of the mesh can be finely adjusted using a mechanism. The frame incorporates a plywood sheet, on which the mounting points of the microphones have been laser cut to ensure that the locations of the microphones are accurate. On the top of the plywood, a layer of polypropylene acoustic foam has been installed. The use of the porous layer is supposed to dampen any standing waves occurring between the wire mesh and the plywood. Figure 9 shows a test, when a stripe of wire mesh was stretched on the frame to find the longest elongation it can withstand.

The preliminary commissioning of the array was performed in a non-echoic condition. In the testing process, the array was used for noise mapping of (a) a single speaker and (b) two speakers, both of which were emitting white noise signals. These tests formed the basis to investigate the performance of the array (dynamic range and the level of sidelobes), which were

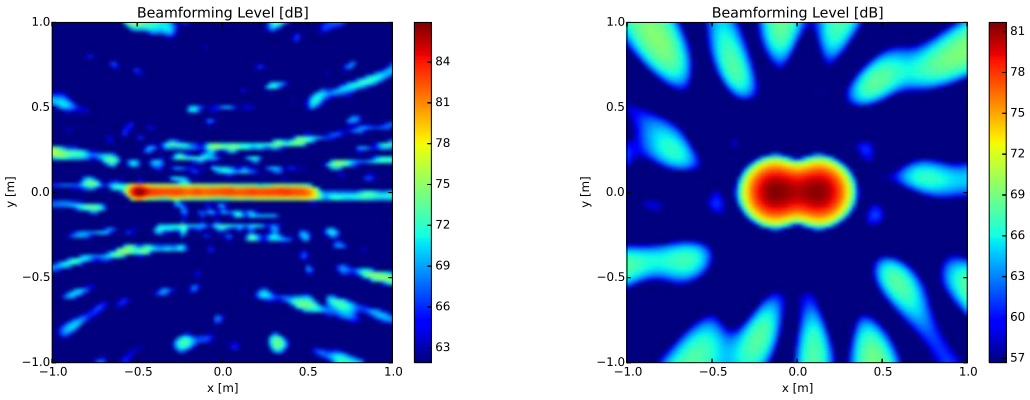

(a) Two noise sources emitting wite noise: beamforming map shown at 8 kHz

(b) Raleigh resolution limit at 1800 Hz for two sources

Figure 8: Simulated results of the best performing array

then compared to the simulations presented in Section 2. The final state of the array is shown in Fig. 10.

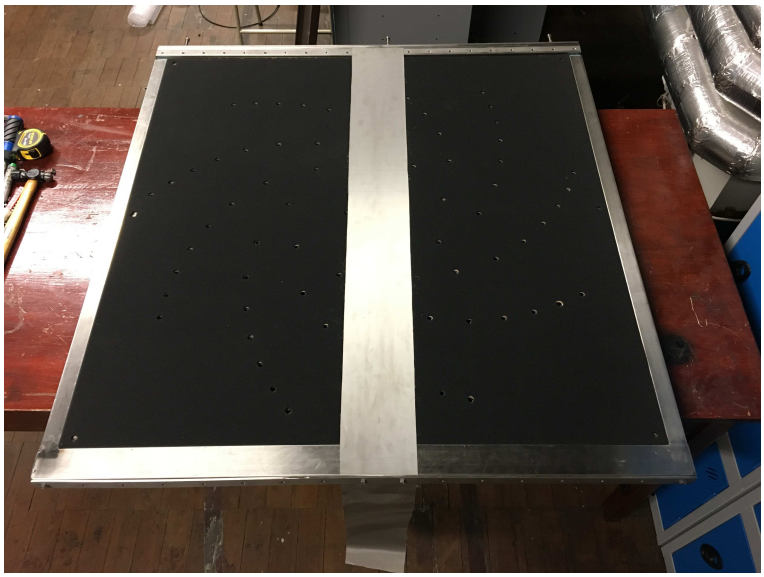

Figure 9: The array with a sample of wire mesh installed on it

The results were post-processed within the Acoular beamforming package, where several beamforming algorithms have been tested (delay-and-sum, DAMAS [5], orthogonal [14] and functional [7]), out of which the results obtained using the delay-and-sum and the functional beamforming are presented here. The exponent term used in functional beamforming algorithm is denoted by γ in the current study, see [7] for more details. All the maps presented in this section show the deviation of the beamforming levels compared to the peak resolved value, which is denoted as the normalized beamforming level (BFL) in the followings. The data was

Figure 10: The array in its final condition

collected for 16 seconds and the sampling frequency was 65,536 Hz (= 2^{16} Hz) in each case. The window length of the Fourier transforms was set to 128 samples.

The speakers were located $2D$ (1.8 m) from the array for both the single and two speakers test cases. The results in Fig. 11 show the comparison of the delay-and-sum and functional beamforming methods for a single point source, evaluated at 8 kHz. It can be seen that the dynamic range of the array for this configuration is in the range of 14-15 dB, while the sidelobes have low amplitude and they are located farther from the noise source than those observed previosuly in the simulations in Section 2. Figure 11(b) shows that the sidelobes can be further eliminated and the source location can be sharpened with the use of functional beamforming, using an exponent of $\gamma = 18$ (see Ref. [7] for the definition).

As a next step, two speakers have been used to create two noise sources, such that they were seen 15° apart from each other from the centre of the array. Figure 12 shows the same comparison of the different methods as in the single speaker case. The dynamic range remained approximately the same as before, while the noise sources spread over a smaller area in this test case for the delay-and-sum beamforming. As observed, the functional beafmorming captures the location of the two noise sources more accurately, i.e. the noise sources spread over a smaller region for this case. The sidelobes have also been successfully eliminated for this case.

As the last step, the two speaker case was investigated at the Raleigh resolution limit, which in this case was 1.8 kHz. The delay-and-sum and the functional beamforming maps were used and the noise map results are presented in Figure 13(a) and 13(b). It can be concluded from the results that the two sources can be hardly distinguished from each other with the use of the conventional beamforming, while using functional beamforming with a higher exponent ($\gamma = 30$), the noise sources become well distinguishable. The functional beamforming maps also

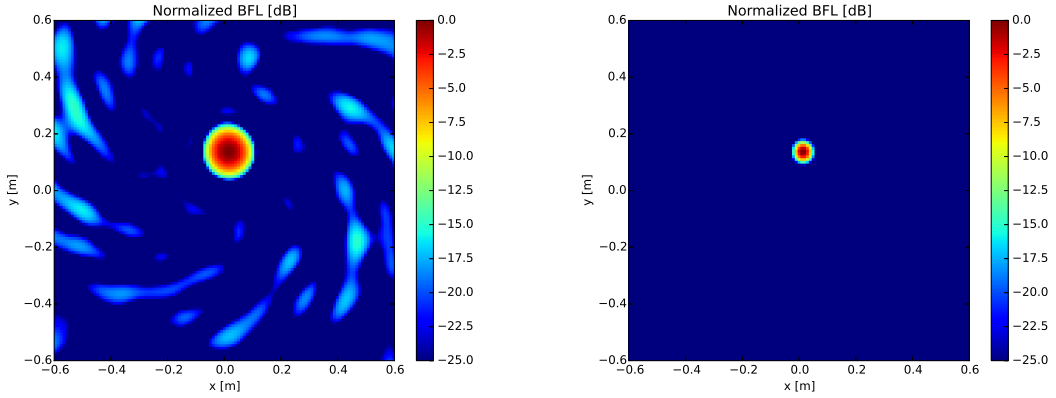

(a) Delay-and-sum beamforming map at 8 kHz (b) Functional beamforming map at 8 kHz, $\gamma = 18$

Figure 11: Single speaker located 1.8 m from the array, different beamforming algorithms

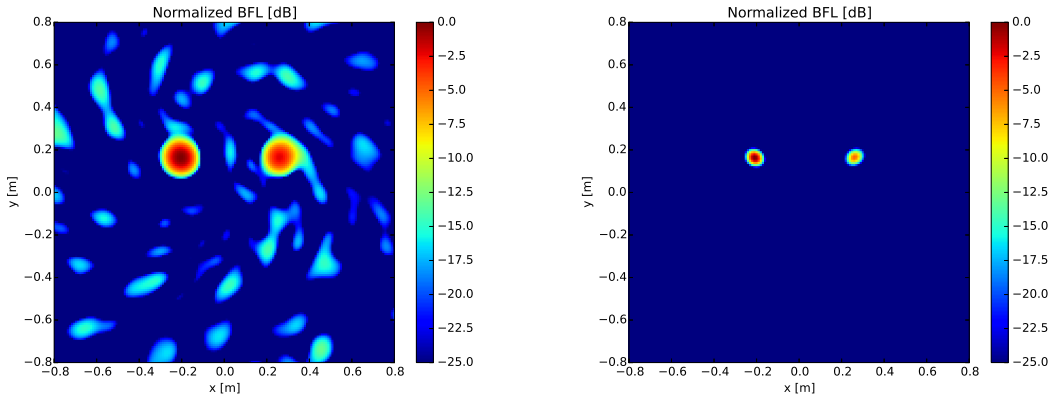

(a) Delay-and-sum beamforming map at 8 kHz (b) Functional beamforming map at 8 kHz, $\gamma = 8$

Figure 12: Two speakers located 1.8 m from the array, seen 15° apart from each other: comparison of different beamforming algorithms

suggests that the amplitude of the left noise source has a lower amplitude, which was caused due to the fact that the amplifiers (two Brüel & Kjaer Type 2706) used in the measurements were slightly different from each other and the gain was adjustable manually.

Based on the presented measurement results, it was concluded that the array can successfully capture the noise source locations, as predicted by the preliminary simulations. Future work will consist of the installation of the array in the De Havilland Wind Tunnel, testing the array for fixed and rotating sources and the in-situ calibration of the array to calculate the exact attenuation caused by the wire-mesh.

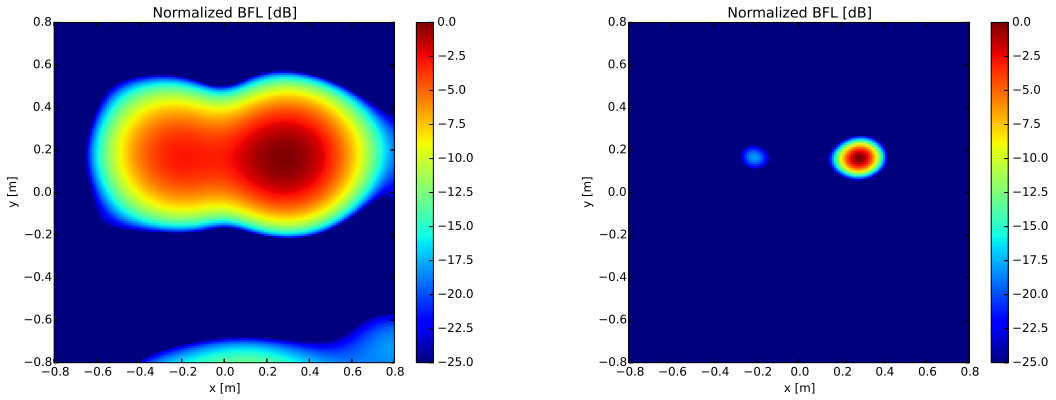

(a) Delay-and-sum beamforming map at 1.8 kHz (b) Functional beamforming map at 1.8 kHz, $\gamma = 30$

Figure 13: Two speakers located 1.8 m from the array, seen 15° apart from each other: comparison of different beamforming algorithms at the Raleigh resolution limit of 1800 Hz

4 SUMMARY

The current paper discusses the design and build of an 80 element beamforming array for helicopter rotor noise measurement purposes within a closed circuit wind tunnel in two steps. In the first step, an effective hydrodynamic noise reduction method is developed, which consists of the recessing of the microphones behind a Dutch twilled woven wire-mesh and the application of acoustic foam in between the two. As a second step, the array design is introduced, where the layout of the microphones in the array is carefully chosen by performing various acoustic simulations, followed by the assembly and testing of the array.

With regard to the hydrodynamic noise reduction, three different woven wire-meshes with different pore sizes and shapes have been investigated. It was found that the use of wire-meshes with smaller pore sizes leads to greater reduction of the hydrodynamic noise. Three different recess depths of the microphones were also investigated (2, 7 and 12 mm), from which the second case was found to give the best results. Finally, the acoustic transparency of the mesh was found to be within a range of 2-3 dB, which was in agreement with the previously published studies.

The layout of the array was chosen using a parametric study for the location of the microphones for different type of noise sources. The array layout is based on a number of widely used logarithmic arms along which the microphones were distributed with an inner and outer radii weighting. Increasing the population of the microphones at the inner and outer radius resulted in higher dynamic range and lower number of sidelobes compared to the layouts where the microphones are distributed with an equal arc-length along the logarithmic arms. The best results were obtained from an array with 9 arms and 8 microphones distributed on each arm, with an extra 8 sensors populated at the centre of the array. A dynamic range up to 15 dB has been achieved using this array.

ACKNOWLEDGEMENTS

This research work has been carried within the framework of the Rotor Rig project, funded by ATI and coordinated by the Aircraft Research Association Ltd. (ARA Ltd.). The authors are grateful to Dr. Csaba Horváth for the useful discussions on beamforming.

REFERENCES

[1] "Acoular – acoustic testing and source mapping software." URL http://www.acoular.org/, accessed 15/Feb/2016.

[2] C. S. Allen, W. K. Blake, R. P. Dougherty, D. Lynch, P. T. Soderman, and J. R. Underbrink. *Aeroacoustic Measurements*. Springer, 2002.

[3] C. S. Allen, K. Vandra, P. T. Soderman, and L. Olson. "Microphone Corrections for Accurate In-Flow Acoustic Measurements at High Frequency." *1st Joint CEAS/AIAA Aeroacoustic Conference, Munich, Germany*, 1995. URL http://ntrs.nasa.gov/search.jsp?R=20010125137.

[4] R. V. Barrett. "Design and Performance of a New Low Turbulence Wind Tunnel at Bristol University." *Aeronautical Journal*, 88(873), 86–90, 1984.

[5] T. F. Brooks and W. M. Humphreys. "A deconvolution approach for the mapping of acoustic sources (DAMAS) determined from phased microphone arrays." *Journal of Sound and Vibration*, 294(4-5), 856 – 879, 2006. ISSN 0022-460X. doi:http://dx.doi.org/10.1016/j.jsv.2005.12.046. URL http://www.sciencedirect.com/science/article/pii/S0022460X06000289.

[6] N. J. Burnside, S. M. Jaeger, B. R. Reinero, W. C. Horne, and P. Soderman. "Array design and performance for a large scale airframe noise study." *8th AIAA/CEAS Aeroacoustics Conference & Exhibit*, 2576, 2002.

[7] R. P. Dougherty. "Functional Beamforming." *Proceedings of the Berlin Beamforming Conference*, 2014. URL http://bebec.eu/Downloads/BeBeC2014/Papers/BeBeC-2014-01.pdf.

[8] V. Fleury, L. Coste, R. Davy, A. Mignosi, C. Cariou, and J.-M. Prosper. "Optimization of Microphone Array Wall Mountings in Closed-Section Wind Tunnels." *AIAA Journal*, 50(11), 2325–2335, 2012. URL http://arc.aiaa.org/doi/pdf/10.2514/1.J051336.

[9] GKD UK Ltd. URL http://gkd.uk.com/, accessed 15/Feb/2016.

[10] W. C. Horne and N. J. Burnside. "Innovative, Low-Cost Phased Microphone Array Design for Moderate-Scale Aeroacoustic Tests." Technical report, NASA, 2014. URL http://nari.arc.nasa.gov/sites/default/files/Horne_s12_7_31_14_0.pdf.

[11] C. Horvath, E. Envia, and G. G. Podboy. "Limitations of Phased Array Beamforming in Open Rotor Noise Source Imaging." Technical report, NASA Technical Report, 2013. URL http://ntrs.nasa.gov/archive/nasa/casi.ntrs.nasa.gov/20140002783.pdf.

[12] S. M. Jaeger, W. C. Horne, and C. S. Allen. "Effect of Surface Treatment on Array Microphone Self-Noise." *AIAA Journal*, 1937, 2000.

[13] P. A. Ravetta, R. A. Burdisso, and W. F. Ng. "Phased Array Technology Development at Virginia Tech: Application to Landing Gear Noise Source identification." *Mecanica Computacional*, 23, 2721–2732, 2004. URL http://www.cimec.org.ar/ojs/index.php/mc/article/viewFile/410/394.

[14] E. Sarradj. "A fast signal subspace approach for the determination of absolute levels from phased microphone array measurements." *Journal of Sound and Vibration*, 329(9), 1553–1569, 2010.